Palaeogeography, Palaeoclimatology, Palaeoecology 371 (2013) 45–53

Contents lists available at SciVerse ScienceDirect

Palaeogeography, Palaeoclimatology, Palaeoecology

journal homepage: www.elsevier.com/locate/palaeo

Reconstructing El Niño-Southern Oscillation activity and ocean temperature seasonality from short-lived marine mollusk shells from Peru

Matthieu Carré [a,*], Julian P. Sachs [b], Andrew J. Schauer [c], Walter Elliott Rodríguez [d], Fredy Cardenas Ramos [e]

[a] UM2-CNRS-IRD, Institut des Sciences de l'Evolution de Montpellier, Université Montpellier 2, CC065, Pl. Eugène Bataillon, 34095 Montpellier, France
[b] University of Washington School of Oceanography, Box 355351, Seattle, WA 98195, USA
[c] University of Washington Department of Earth and Space Sciences, Box 351310, Seattle, WA 98195, USA
[d] IMARPE, Laboratorio Costero de Huacho, Avenida San Martin 710 Carquín, Huacho, Peru
[e] IMARPE, Laboratorio Costero de Ilo, Ilo, Peru

ARTICLE INFO

Article history:
Received 18 June 2012
Received in revised form 30 November 2012
Accepted 12 December 2012
Available online 28 December 2012

Keywords:
Eastern tropical Pacific
ENSO
Paleoclimate
Sea surface temperature
Mollusk
Stable isotopes

ABSTRACT

A critical need exists for quantitative reconstructions of long-term El Niño Southern Oscillation (ENSO) variability in the eastern tropical Pacific. Presented here is a method to quantitatively estimate past changes 1) in the seasonal amplitude of sea surface temperature (SST) in the Peruvian coastal upwelling system and 2) in the amplitude of ENSO-related interannual variability in the eastern tropical Pacific. The seasonal amplitude of SST (ΔT) along the length of the Peruvian coast is strongly correlated with the Niño1 + 2 index. We show that the frequency distribution of ΔT values provided by a modern sample of 13 *Mesodesma donacium* shells faithfully reflects modern ENSO variability at the regional scale, including the range of anomalies from La Niña to moderate El Niño events, but excludes extreme warm anomalies because of high shell mortality. We propose to use the frequency distribution of ENSO anomalies in paleoclimate studies for comparisons between shell records, coral records, and GCM simulations. Reconstruction uncertainties can be quantified using Monte Carlo simulations. The method presented here opens new perspectives for quantitative paleo-ENSO reconstructions in the Eastern Pacific since it may be applied with any mollusk species from Peru provided at least one annual cycle of SST is faithfully recorded by shell $\delta^{18}O$.

1. Introduction

Reconstructing a long-term record of El Niño Southern Oscillation (ENSO) is critical to identify the forcings that influence its activity and to estimate its sensitivity to global climate change. Past changes in ENSO variability not only involve changes of the event intensity and frequency, but also changes in the distribution of cold and warm events, and changes in the spatial pattern of sea surface temperature (SST) anomalies. This means that records of interannual SST are needed from across the tropical Pacific, from the warm pool to the cold tongue, to properly evaluate past ENSO modes.

So far, proxy records of the tropical Pacific SST with seasonal resolution have been obtained primarily from Sr/Ca and $\delta^{18}O$ analyses of coral (Cole and Fairbanks, 1990; Dunbar et al., 1994; McCulloch et al., 1996; Corrège et al., 2000; Tudhope et al., 2001; Evans et al., 2002; Cobb et al., 2003; Kilbourne et al., 2004; McGregor et al., 2010). Fossil corals faithfully record past interannual climate variability in the Pacific warm pool and in the central Pacific but they are very scarce in the eastern tropical Pacific. The most ancient coral analyzed in the eastern tropical Pacific was collected in the Galapagos Islands and reached 1587 A.D. (Dunbar et al., 1994).

On the eastern side of the Pacific, most paleoclimate studies dedicated to ENSO reconstruction for long intervals are based on rainfall proxies of the American continent (D'Arrigo and Jacoby, 1992; Stahle et al., 1998; Rodbell et al., 1999; Moy et al., 2002; Riedinger et al., 2002; D'Arrigo et al., 2005; Rein et al., 2005; Conroy et al., 2008). However, all these signals are communicated through atmospheric teleconnections that are likely to change over time. Changes in the rainfall regime may also be linked to changes in the intensity or in the seasonal movement of the intertropical convergence zone (ITCZ). In the tropical Andes, the Atlantic Ocean and the South American monsoon system also have a large influence on rainfall variability (Garreaud et al., 2009). Consequently, rainfall-related paleoclimate records provide valuable data for the study of continental rainfall variability but yield only indirect and often mixed information for past ENSO activity.

Marine indications for past changes in ENSO activity in the eastern tropical Pacific have been obtained from the variance of individual foraminifera $\delta^{18}O$ values in marine sediment samples (Koutavas et al., 2006; Leduc et al., 2009). Since marine cores have a centennial resolution and foraminifera live about a month, the variance of a foraminifera sample yields a mixed signal that involves temperature

* Corresponding author. Tel.: +33 4 67 14 38 08; fax: +33 4 67 14 40 44.
E-mail address: matthieu.carre@univ-montp2.fr (M. Carré).

0031-0182/$ – see front matter © 2013 Elsevier B.V. All rights reserved.
http://dx.doi.org/10.1016/j.palaeo.2012.12.014

seasonality, temperature gradient in the mixed layer, ENSO-related interannual variability, and multidecadal variability.

Here we present a technique that responds to the critical need for quantitative estimates of the marine interannual variability in the eastern tropical Pacific. We show how short-lived marine mollusk shells, despite the brevity of their timespan, can be used as a paleoclimate archive for reconstructing the seasonal range of SST and ENSO variability in the tropical Pacific cold tongue, and how these data can be compared to coral records and model outputs. The technique shares similarities with the coral-based approach since it involves short high resolution windows at a monthly time scale, but also with the individual foraminifera technique since paleoclimate is estimated by the statistics of a random sample. The advantage of the mollusk-based technique compared to foraminifera is that it allows independent reconstruction of the seasonal cycle and more comprehensive characterization of ENSO variance.

It has been previously established that marine mollusk shell $\delta^{18}O$ may be a reliable SST proxy as long as water $\delta^{18}O$ can be reasonably constrained (Grossman and Ku, 1986; Hickson et al., 1999; Schöne et al., 2004). On the Peruvian coast, the monthly sea water $\delta^{18}O$ variations are very small (typically <0.1‰) because precipitation is virtually nonexistent and river discharge is minimal, so that mollusk species such as *Mesodesma donacium* faithfully record coastal SST variations at a monthly time scale over 1–3 year long windows (Carré et al., 2005). Although continuous records of at least several decades are generally preferred to study ENSO variability, we will examine here how a discontinuous sample of short-lived shells from Peru can also yield a reliable statistical estimate of ENSO variability.

We will examine the relationship between coastal SSTs in the Peruvian upwelling system and the Niño1 + 2 index to assess the spatial range of representativeness of coastal records. Uncertainties will also be quantitatively assessed using the MoCo program (Carré et al., 2012). Our approach, presented here with one species, is valid for any coastal mollusk species that faithfully records at least one annual SST cycle. Our study potentially opens new opportunities for direct and quantitative paleo-ENSO reconstructions in the eastern tropical Pacific, using anthropogenic or natural fossil shell accumulations in Peru.

2. Materials

M. donacium is an endemic intertidal bivalve species of Peruvian and Chilean sandy beaches that has been gathered for food since the first human occupation of the Peruvian coast (Sandweiss et al., 1989, 1998; Carré et al., 2009; Lavallée et al., 2011). In 1980, the northern limit of *M. donacium* was 10°S in Sechura Bay (Tarifeño, 1980). Its distribution today is restricted to south of ~15°S because of mass mortality induced by the extreme El Niño events of 1983 and 1998 (Riascos et al., 2009). This means that *M. donacium* shells cannot record extreme warm anomalies (9.5 °C in 1983 and 8.8 °C in 1998 in Puerto Chicama). After the 1983 event, populations recovered within a few years but the 1998 event had a much more prolonged impact since populations have not fully recovered so far, 15 years after the mortality event, perhaps because of competition or changes in the beaches slope and granulometry. Some periods following similar extreme events might therefore not exist in the fossil record but such potential gaps are not expected to produce any bias since there is no evidence that ENSO activity may be systematically stronger or weaker during the decade following an extreme event.

A sample of 13 *M. donacium* shells was collected in 2007 from modern shell mounds behind the long sand beach close to the Ica River mouth (14°52′19″S; 75°33′21″W) (Fig. 1). Based on fishermen testimonies and newspaper fragments found in shell mounds, we know that these shells were gathered by fishermen during the last decades of the 20th century, when these surf clams were a significant economical resource. These shells cannot be cross-dates. To minimize the probability of collecting shells from the same year, every shell was collected in a separate mound. This modern shell sample thus represents a random sample of 13 short-term windows which combined represent the environmental conditions during the last decades of the 20th century. In this, our modern sample would mimic shell samples from archeological middens and could therefore be used as a modern reference.

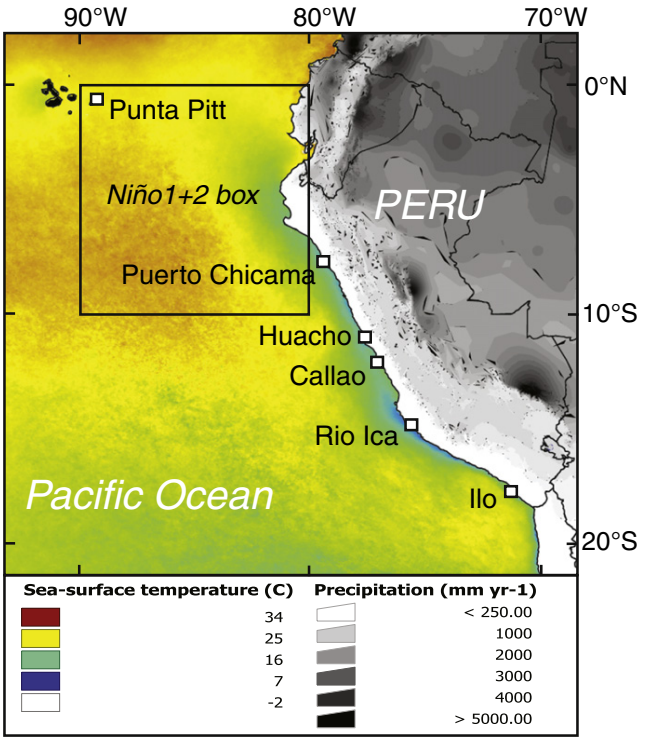

Fig. 1. Map of the study area with mean annual SST and annual precipitation on the continent. The Niño1 + 2 area and the sites mentioned in the text were indicated.

3. Methods

3.1. Microsampling and isotopic analyses

Radial shell sections were polished and serially microsampled in the outer layer using an automated microdrilling system (Micromill, Merchantek™) with a three-edged pyramidal dentist drill. Microsamples consisted in a ~0.15 mm deep and ~0.2 mm wide groove and were adjacent for a continuous sampling (Fig. 2). Based on shell growth lines, the length of the groove was adapted to the growth rate so the sample would integrate about a month.

The oxygen isotopic composition of powdered aragonite microsamples (~50 μg) was analyzed at the University of Washington Isolab using a Finnigan Delta Plus isotope ratio mass spectrometer coupled to a Kiel III carbonate device. Aragonite samples were digested in 100% phosphoric acid at 70 °C. The standard deviation for repeated measurements of the internal standard was better than 0.08‰. Raw $\delta^{18}O$ values were corrected as per Tobin et al. (2011) for temperature-induced isotopic drift observed in micromilled aragonite (−0.1‰/day at 70 °C). $\delta^{18}O$ values were reported with respect to the Vienna Pee Dee Belemnite (VPDB) scale using NBS19 ($\delta^{18}O = -2.2$‰) and NBS18 ($\delta^{18}O = -23.01$‰) (Coplen, 1996). Data points corresponding to seasonal extrema were re-sampled on the shell and re-analyzed. Values from replicate microsamples were then averaged. Isotopic values were not corrected for the difference of CO_2-acid fractionation factors between calcite and aragonite

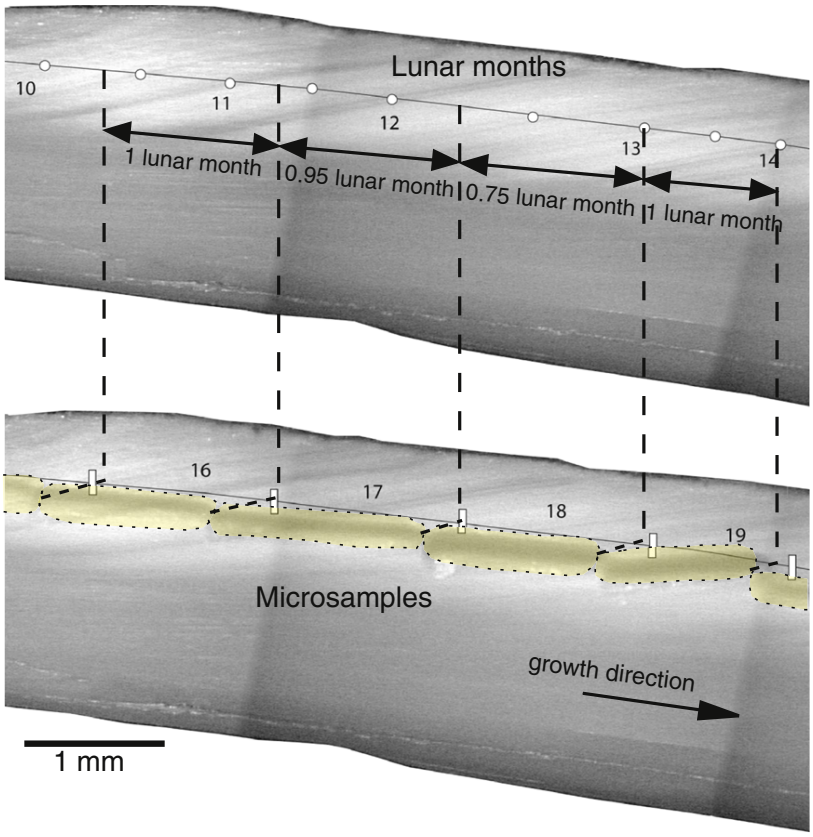

Fig. 2. Detail of Ica-3 shell section illustrating the method used to determine subannual chronology of shell isotopic records. Top: polished section showing fortnightly growth lines (open circles on an arbitrary line following the growth axis) and numbers of lunar months from the microsampling starting point. Bottom: same section after microsampling. Microsample grooves were indicated in yellow and numbered. Their limits were indicated by open rectangles on the same growth axis. Time intervals represented by microsamples were estimated on the growth axis in the top section by the intervals between vertical dotted lines.

(Kim et al., 2007) because paleotemperature equations mentioned further in the text were calculated with uncorrected values (Grossman and Ku, 1986; Carré et al., 2005).

Sea water samples were collected from the surface water close to the shoreline in glass vials avoiding the presence of air bubbles. Vials were sealed with tape and stored at 5 °C. Water $\delta^{18}O$ values were analyzed by mass spectrometry using the classical CO_2–H_2O equilibration method (Cohn and Urey, 1938), with a precision of ±0.1‰. Seawater samples were equilibrated for 8 h at 40 °C. Water oxygen isotope ratios are reported with respect to Vienna Standard Mean Ocean Water (VSMOW).

3.2. Shell inner chronology and seasonal extrema

Polished shell sections were observed and photographed with a binocular microscope under reflected light. In fast growing parts of *M. donacium* shells, thin growth lines can be observed that were shown to be produced during daily low tides (Carré et al., 2005). These lines form darker clusters during spring tide periods with a fortnightly periodicity. These fortnightly growth lines were used in a first phase to keep microsampling resolution close to one month. There is, however, uncertainty in the identification of these fortnightly lines due to the pattern variability (Carré, 2007; Carré et al., 2009). Subannual chronology was thus more precisely determined during a second phase combining isotopic records with growth lines. In a simultaneous process, we defined seasonal extrema, and selected the sclerochronological reading that would allow them to be separated by ~12 ± 1 months. Based on this adjusted interpretation of shell growth lines, the timespan of every microsample was calculated (Fig. 2), and shell isotopic records were plotted on a monthly time axis (Fig. 3). Local extrema related to the strong intra-seasonal variability on the Peruvian coast rather than to the annual cycle could be discriminated in this process (for example in shells Ica-3 and Ica-4, Fig. 3). Temporal resolution of the records ranged from ~0.5 to 3 months. The average resolution of the whole record was 1.2 months ($\sigma = 0.5$ months). There was no systematic bias in time resolution related to growth rate changes since microsampling resolution was adjusted growth rate. The lowest resolution in extrema values was 2.5 months. The seasonal amplitude of shell $\delta^{18}O$ represents the seasonal amplitude of SST (ΔT) and was taken to be the difference between the summer maximum and the winter minimum that preceded or followed it (Fig. 3). First or last data points were not used for the calculation of seasonal amplitudes unless the shell chronology showed a time difference with the closest minimum (maximum) larger than 12 months.

3.3. Estimation of uncertainties

Shell isotopic records converted to SST using a paleotemperature equation (Grossman and Ku, 1986; Carré et al., 2005) provide a statistical estimate of the average and variance of the seasonal amplitude of the SST (ΔT) for the late 20th century. The systematic and standard error associated to this estimate was quantified by a Monte Carlo simulation using the MoCo program, that simulates the uncertainty sources of mollusk- and coral-based SST reconstructions (Carré et al., 2012). MoCo was parameterized here to mimic the uncertainty sources specific to *M. donacium*, which includes a range of temperature from 6 to 22 °C for shell growth (temperatures over 22 °C are

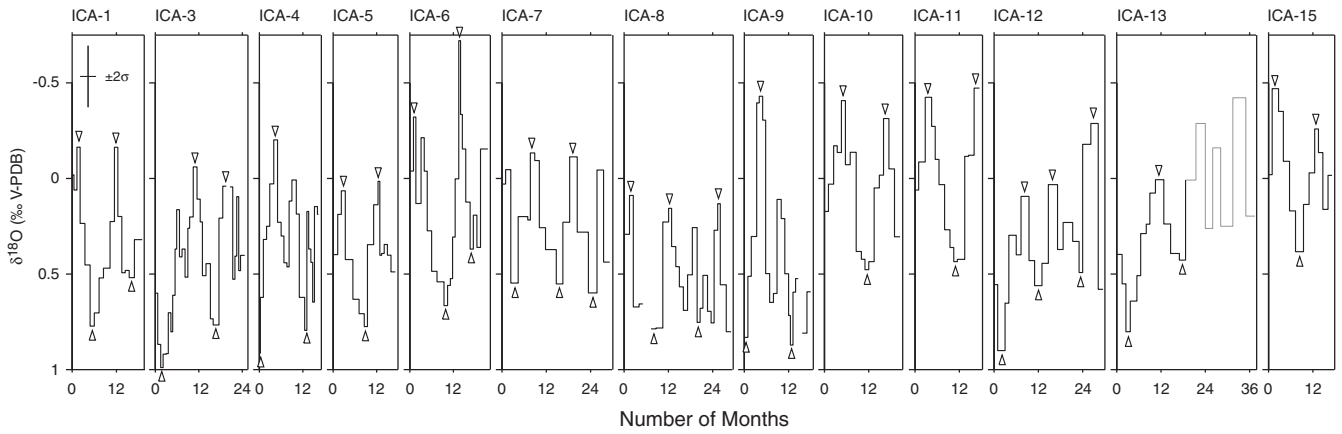

Fig. 3. $\delta^{18}O$ profiles of 13 modern *Mesodesma donacium* shells from the Rio Ica site, on monthly time axis. The length of horizontal segment represents the duration averaged by shell microsamples. Line interruptions are due to loss of samples. Gray line in Ica 13 indicates the part of the isotopic signal where the resolution was too low to accurately estimate seasonal amplitudes. Open triangles indicate seasonal extrema that were used for the calculation of ΔT values. These data points were averaged from at least 2 replicate analyses.

thus not recorded), random growth breaks, spatial heterogeneity of the coast, monthly variability of water $\delta^{18}O$, and analytical standard error for isotopic ratio. Temporal resolution variability in shell records is also a source of uncertainty for estimating ΔT, but is not included in MoCo simulations. The standard error was calculated as the standard deviation of the population of errors obtained by iterated reconstruction simulations. The instrumental temperature time series of Puerto Chicama was used for the simulation and error calculation. Extreme Niño years 1982–83 and 1997–98 were removed for an adequate assessment of uncertainties since the species does not record this part of ENSO variability. The uncertainty analysis is therefore assessing the ability of a shell sample to record the range of ENSO variability from La Niña anomalies to "normal" El Niño anomalies. The complete parameterization is available in the online Supplementary material.

4. Results and discussion

4.1. Variability of sea water $\delta^{18}O$

Sea water salinity and $\delta^{18}O$ are strongly correlated on monthly to decadal time scales since their variations are both dictated by freshwater input and evaporation (Epstein and Mayeda, 1953; Fairbanks et al., 1982). Salinity variability can therefore provide reliable indications about water $\delta^{18}O$ variability when direct isotopic data are not available. We compared monthly salinity time series for the period 2000–2007 from three IMARPE coastal laboratories, Huacho, Callao, and Ilo (Fig. 4). In the three sites, salinity variations were very small, with standard deviations of 0.11, 0.11, and 0.07 respectively (Fig. 4A). Although there was a slight tendency for higher salinity values during austral summer, the mean annual cycle was very weak, with amplitudes of 0.23, 0.09, and 0.06 respectively, which are similar to the monthly standard deviation. By extension we infer that coastal water $\delta^{18}O$ variations on intra- and inter-annual time scales are small on the central and southern coast of Peru. This result was confirmed by monthly time series of water $\delta^{18}O$ obtained in 2003 in Huacho and in 2003–2004 in Ilo (Fig. 4B). In these two short records, the standard deviation of sea water $\delta^{18}O$ was 0.2‰ and 0.14‰ respectively, but no seasonal signal could be discerned. These water isotopic values, however, do not faithfully reflect the monthly variability because they are instantaneous measurements and include thus a daily variability. The long series of monthly salinity data provide a better estimate of the isotopic monthly variability because they are averaged values of daily to weekly measurements. Based on Fairbanks' et al. (1982) relationship between salinity and water $\delta^{18}O$ in the eastern tropical Pacific, a standard deviation of 0.11 for salinity corresponds to a standard deviation of 0.03‰ for water $\delta^{18}O$, which translates into an uncertainty of ~0.1 °C for SST estimates. These data confirm that the intra-seasonal variations of water $\delta^{18}O$ do not significantly affect the reconstruction of seasonal SST variations. This result is also valid for the study site since the nearby Ica River has a small discharge that cannot significantly affect the sea water isotopic composition for a period as long as a month. In the exceptional case that the river flow was strong enough to affect the sea water $\delta^{18}O$, this type of event would be detected in the isotopic shell record by a simultaneous drop in both $\delta^{18}O$ and $\delta^{13}C$ values. This was not observed in modern Ica shells. A value of 0.05‰ was used for water $\delta^{18}O$ monthly variability in MoCo simulation. Sea water $\delta^{18}O$ also varies on millennial time scales with polar ice volume. This would affect the reconstruction of absolute temperatures but not of ΔT values which is used here to estimate ENSO activity as we will show in Section 4.3.

Mean sea water isotopic composition shows some geographical variations along the coast (Fig. 4C,D). A mean sea water $\delta^{18}O$ value of 0.24 ± 0.11‰ for the study area was estimated from 12 sea water samples taken along the coast between Callao (12°04′S) and Tanaka (15°43′S) at different times from 2001 to 2007. The sea water $\delta^{18}O$ values with the precise locations and dates of sampling are available in the online Supplementary material.

4.2. Shell $\delta^{18}O$ profiles

We obtained 13 isotopic records ($\delta^{18}O$) spanning one to two years with approximately 1-month resolution (Fig. 3). The cumulated timespan of the 13 shells is about 25 years assuming nonredundancy. The microsampling resolution ranged from 0.5 to 2 lunar months, except in the last part of shell Ica-13 which was not used for seasonality estimates because the timespan of microsamples was larger than 2 months. Single shell mean values ranged from −0.04‰ to 0.51‰ while the mean $\delta^{18}O$ value for the whole dataset was 0.25‰ (N = 249 data points).

Considering a sea water $\delta^{18}O$ value of 0.24‰ and using the paleotemperature equation calculated by Carré et al. (2005) for *M. donacium*, mean SST values calculated for single shells ranged from 16.5 °C to 18.5 °C, whereas the mean SST calculated for the full dataset was 17.4 °C. This value is in good agreement with the NODC (Levitus) World Ocean Atlas 1994 (Monterey and Levitus, 1997) (0.25° gridded dataset provided by the NOAA/OAR/ESRL PSD, Boulder, Colorado, USA, from their Web site at http://www.esrl.noaa.gov/psd/.) that indicates

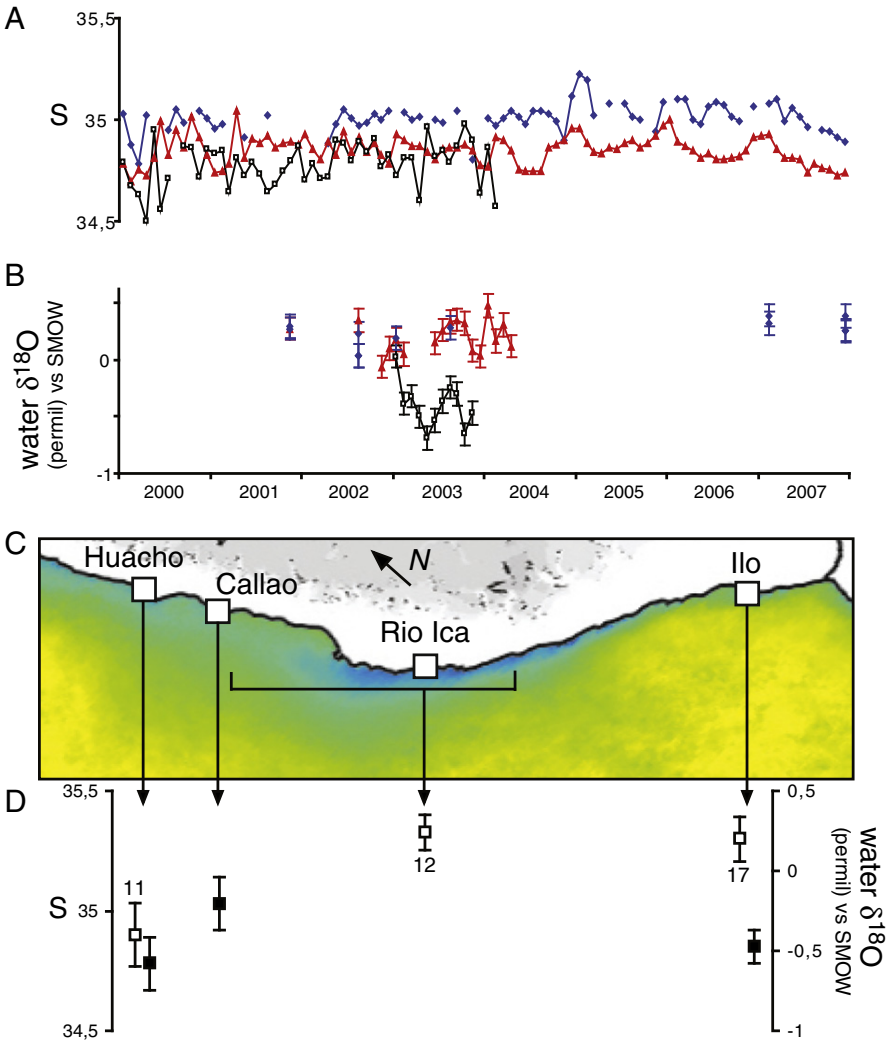

Fig. 4. A: Monthly time series of surface salinity in Huacho (open squares), Callao (blue diamonds), and Ilo (red triangles) measured by IMARPE. B: Sea water $\delta^{18}O$ data from Huacho (open squares), Ilo (red triangles), and coastal sites from the Rio Ica area (from Callao to Tanaka) (blue diamonds). Precise dates and locations were listed in Supplementary material. C: Legend as in Fig. 1. D: Mean values and standard deviation of salinity (black squares) and sea water $\delta^{18}O$ (open squares) for the locations indicated by arrows on the Peruvian southern coast.

mean annual SSTs from 17.2 to 17.7 °C along the Peruvian coast between 14°S and 16°S.

The seasonal amplitude of $\delta^{18}O$ was converted to a seasonal amplitude of SST and will be referred to as ΔT values thereafter. Each shell yielded between 2 and 4 ΔT values. 36 ΔT values were calculated from the full dataset with an average value of 3.0 °C using an aragonite temperature-fractionation slope of −3.66 °C/‰ (Carré et al., 2005) or 3.5 °C using a slope value of −4.34 °C/‰ (Grossman and Ku, 1986). These values are close to the mean seasonal amplitudes calculated from instrumental SST time series of Callao (3.5 °C) and Ilo (3.2 °C), implying that seasonal temperature variations are faithfully recorded by the shells. However, mollusk ΔT mean value calculated from Grossman and Ku's (1986) slope is closer to the Callao instrumental value while Carré et al.'s (2005) slope yields a value closer to Ilo instrumental value. Since our site is geographically closer to Callao and until further data from Rio Ica is available, we choose to use here Grossman and Ku's (1986) temperature-fractionation slope for the calculation of ΔT. The standard errors of the shell-derived mean SST (Tm) and mean ΔT value (<ΔT>) are ±0.36 °C and ±0.28 °C respectively for this sample size, based on Monte Carlo simulations with the MoCo program (Carré et al., 2012) (Fig. 5). These simulations also suggest that there is no systematic bias in the estimate of the annual mean temperature but a slight overestimation of 0.27 °C for <ΔT> (Fig. 5). This bias is due to the combined effect of monthly water $\delta^{18}O$ variability, carbonate microscale isotopic heterogeneity, and analytic uncertainty (Carré et al., 2012).

4.3. ENSO and the seasonal cycle of SST on the Peruvian coast

Coastal conditions may not be representative of the open ocean, especially where strong upwelling occurs, as in Peru. We aimed to test if paleoceanographic results from the Peruvian coast could be compared with results obtained from sediment cores or with climate model outputs. We thus examined how coastal SSTs in Peru correlate with the Niño1+2 index (0–10°S, 90–80°W) (Fig. 6). The direct month-to-month Pearson correlation coefficient between Niño1+2 index and *in situ* SST anomaly time series from Puerto Chicama (7°42′S), Callao (12°04′S), and Ilo (17°38′S) were respectively 0.85, 0.75, and 0.75 (Fig. 6A). Despite the long distance (~2000 km from Ilo to the center of Niño1+2 box) and the influence of the coastal upwelling, these high correlation coefficients imply that SST

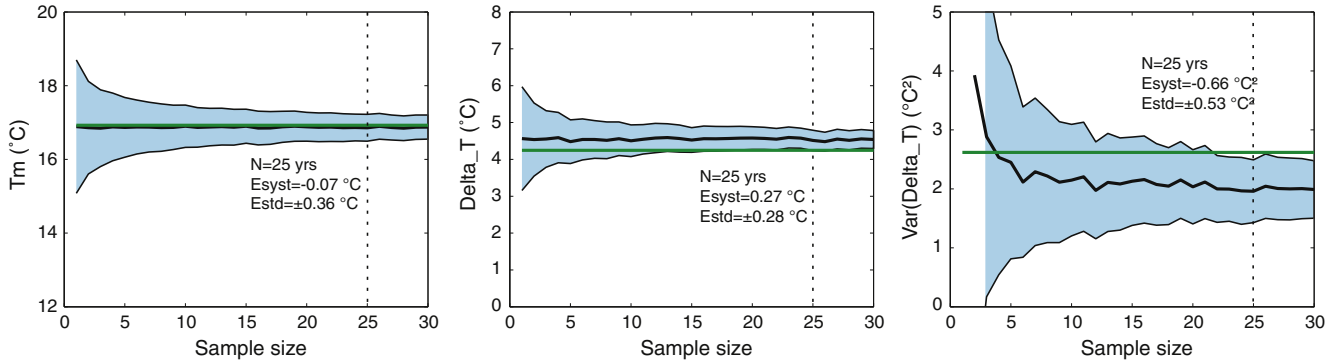

Fig. 5. Monte Carlo simulations of the reconstruction of the annual mean temperature Tm (left panel), the mean SST amplitude (central panel), and the ENSO activity indicated by the variance of the SST seasonal amplitude (right panel) using the MoCo program (Carré et al., 2012). Details about the program parameterization are given in online Supplementary material. Thick black lines indicate the reconstructed value *vs.* the cumulated number of years recorded by a shell sample (here the number of 1-year long shells). The green line shows the true value calculated from the 1925–2002 SST time series of Puerto Chicama, Peru. The blue area limited by thin black lines shows the standard error interval. The dotted line corresponds to the modern shell sample of Ica presented in this study which cumulates *ca.* 25 years. The systematic error values (Esyst) and the standard error values (Estd) obtained for N = 25 years are indicated.

anomalies along the Peruvian coast are likely influenced by the same factors that influence the Niño1 + 2 region. ENSO and warm (El Niño) events in particular are clearly captured by the coastal SST series and Niño1 + 2 (Fig. 6A).

However, absolute SST anomalies (which usually characterize ENSO) cannot be faithfully estimated in individual mollusk records because of the brevity of their lifespan and the local scale variability of mean conditions that prevent us from determining a reliable climate baseline for every single shell. We therefore examined further how the seasonal amplitude of SST on the Peruvian coast was related to ENSO. The correlation coefficients between Niño1 + 2 annual means and instrumental SST seasonal amplitudes in Puerto Chicama, Callao, and Ilo were respectively 0.87, 0.85, and 0.82 (Fig. 6B). This implies that ENSO strongly affects the seasonal amplitude of SST along the length of the Peruvian coast, with large amplitudes indicative of warm events and small amplitudes indicative of cold events. The cause of this relationship is the coastal upwelling that strongly depresses SST anomalies during austral winter so that coastal SSTs are mostly affected by ENSO events (warm or cold) during austral summer when coastal upwelling is lower. As a result, ENSO anomalies can be diagnosed by coastal ΔT anomalies. Since the relationship is linear (Fig. 6B) the variance of ΔT values should be related to the amplitude of ENSO variability in the Niño1 + 2 area. This was confirmed by the strong linear correlation between the variance of the Niño1 + 2 index annual mean and the variance of coastal ΔT values in Puerto Chicama, Callao, and Ilo over the 1950–2002 period (Fig. 6C).

As a result, the variance of ΔT values (Var(ΔT)) calculated from a sample of mollusk shells is a measure of ENSO-related SST variability in the Niño1 + 2 region. <ΔT> and Var(ΔT) (the mean and the variance) of the shell sample from Rio Ica can be used, respectively, as modern references to estimate changes in the SST seasonality and the amplitude of ENSO variability from fossil shell samples of the same species in the same region. Reconstructions of past conditions should be normalized by these modern values. This way, $<\Delta T>_{fossil}/<\Delta T>_{modern}$ and $Var(\Delta T)_{fossil}/Var(\Delta T)_{modern}$ are quantitative estimates of past changes in SST seasonality and ENSO activity, and are independent from the paleotemperature proxy model and its inherent uncertainties. This method could be applied with any Peruvian mollusk species that faithfully records the whole seasonal amplitude of SST, such as *Argopecten purpuratus* (Jones et al., 2009), *Trachycardium procerum* (Perrier et al., 1994; Andrus et al., 2005), and *Protothaca thaca* (Lazareth et al., 2006). Monte Carlo simulations indicate that the standard error for the reconstruction of var(ΔT) with our sample is ± 0.53 °C² (Fig. 5), which represents an uncertainty of ~19%. This uncertainty is much larger than for Tm and <ΔT> which was expected since capturing the variance is much more difficult than capturing average values. A systematic underestimation is also observed primarily due to the shell growth temperature threshold. These results show that reconstructions from fossil samples need to be compared to similar modern samples that will have similar biases.

Fossil shell samples may be collected from natural marine terraces or anthropogenic accumulations. A shell sample from a dated stratigraphical layer yields then a random sample of short-term windows producing together a statistical estimate of average conditions for the time period corresponding to the layer accumulation. Uncertainty related to statistical representativeness of the sample may be estimated using the MoCo program (Carré et al., 2012).

4.4. Characterizing and comparing ENSO records

ENSO activity is generally traced in long continuous proxy records by the interannual band of the frequency power spectra. The amplitude of its variability is then estimated by the variance of the filtered proxy record. We argue here that ENSO activity can also be usefully characterized by the frequency distribution of the ENSO-related anomalies. This simple representation allows better evaluation of changes in the intensity of events and in the distribution between El Niño and La Niña anomalies. The frequency distribution of Niño1 + 2 SST anomalies appears not to be symmetrical (Fig. 7A) as it is in the central equatorial Pacific (not shown). In the eastern Pacific, El Niño anomalies are larger than La Niña anomalies. On the Peruvian coast, Callao ΔT values and mollusk-derived ΔT values have similar asymmetric distributions that were most closely characterized by lognormal distributions (Fig. 7B,D). For better comparison with instrumental records, mollusk-derived ΔT values were calculated from $\Delta\delta^{18}O$ using the temperature calibration of Grossman and Ku (1986), which has a slope of 4.34 °C/‰, but using the slope from Carré et al. (2005) would not change the outcome and the ΔT distribution would still be lognormal.

Extreme El Niño warm events in 1983 and 1998 which represent the two warmest anomalies in the Niño1 + 2 series from 1950 to 2002 (Fig. 7A), were not included in the Callao distribution because *M. donacium* mortality is extremely high at these temperatures and they are therefore not expected to be observed in the fossil record of that species. However, the similarity of the mollusk ΔT distribution with the instrumental ΔT distributions is an additional confirmation that *M. donacium* is a reliable archive of ENSO variability, recording La Niña anomalies to "normal" El Niño anomalies. Given the lognormal form of the distributions, the mode and the threshold for La

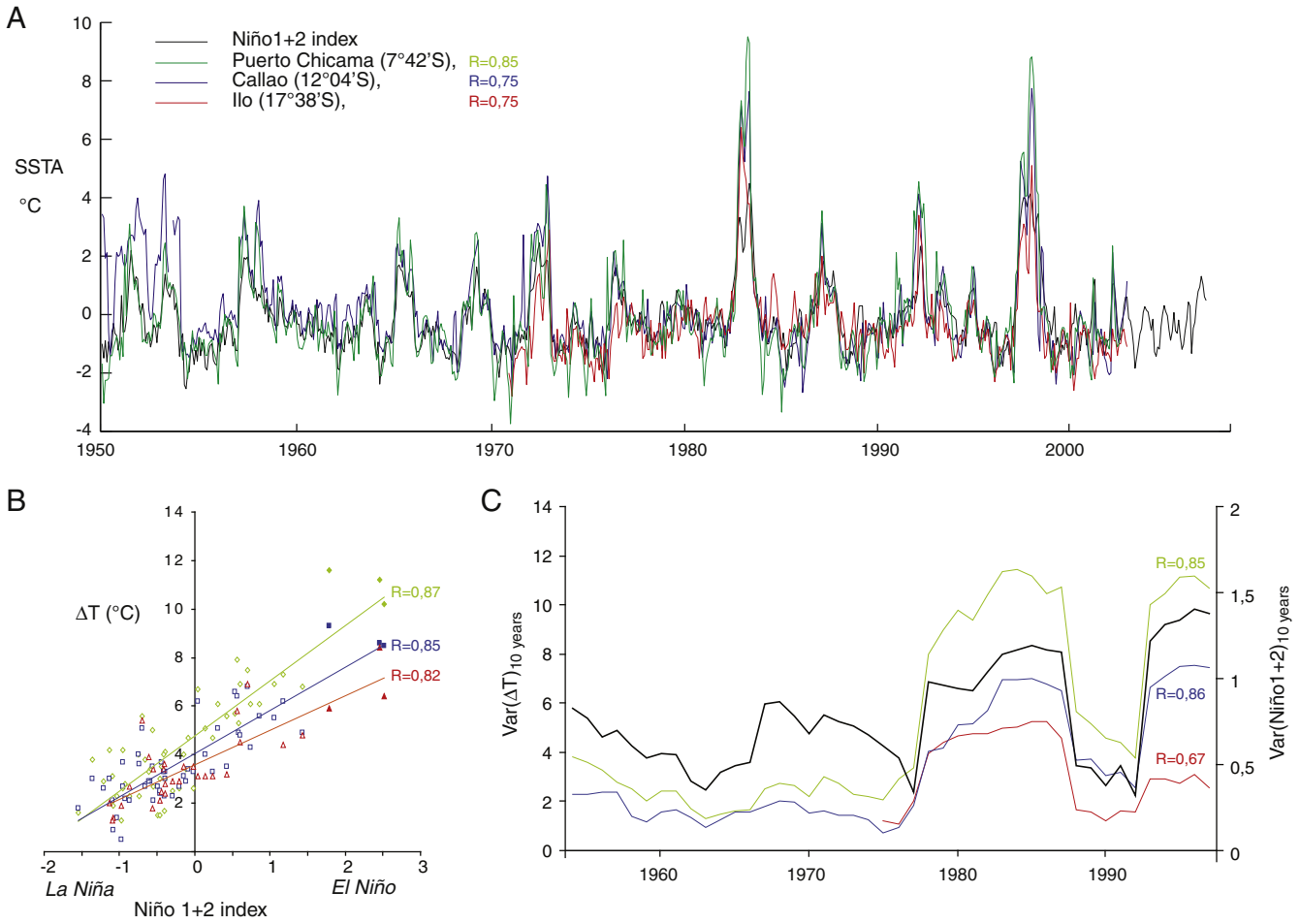

Fig. 6. A: Monthly SST anomalies from the Niño1 + 2 area (black), Puerto Chicama (green), Callao (blue) and Ilo (red). SSTs from Peru were measured *in situ* by IMARPE. Correlation coefficient of the coastal time series with the Niño 1 + 2 series are indicated. B: Linear correlations between Niño1 + 2 index annual mean and ΔT values from Puerto Chicama (green), Callao (blue), and Ilo (red). C: Variance of Niño1 + 2 index in 10-year running windows (black) compared to the variance of ΔT in 10-year running windows in Puerto Chicama (green), Callao (blue) and Ilo (red), with the corresponding correlation coefficients.

Niña and El Niño were defined by the mean and the standard deviation of the normal distributions of Ln(ΔT).

1982–83 and 1997–98 account for 25% of the variance in the Puerto Chicama time series, but this contribution is so dependent on a single event that it may vary significantly. These events were the most significant in terms of impact, and thus focused a lot of attention from the scientific community. However, they are so extraordinary in terms of timing and intensity that they are arguably not representative of the southern oscillation (Takahashi et al., 2011). Although these two events occurred in an interval of 15 years, they are unique in the instrumental record and may have been in the last centuries. Our proxy is thus complementary with rainfall-related proxies because it focuses on the southern oscillation itself while the latter record its occasional catastrophic extensions.

One of the most important results of this study is that a quantitative paleo-ENSO reconstruction method is now available for the eastern Pacific that allows direct comparisons with coral records from the central and western Pacific and with climate model outputs. To illustrate this, we plotted the distribution of the annual mean of Niño1 + 2 index from a 1000-year preindustrial control simulation of the IPSL_CM4v2 coupled ocean atmosphere general circulation model (GCM) (for details about the simulation, see Servonnat et al. (2010)), and the distribution of mean annual $\delta^{18}O$ values from the Punta Pitt coral studied by Shen et al. (1992) (Fig. 7C,E). The IPSL_CM4v2 model yielded a normal distribution and thus failed to capture the characteristics of the observed SST anomaly distribution in the Niño1 + 2 region, as most climate models do. The distribution from the Galapagos coral is slightly asymmetric but much less so than the Niño1 + 2 index distribution, which suggests that this coral may have stopped growing during the largest El Niño events.

5. Conclusions

Seasonal SST variations are faithfully reconstructed from $\delta^{18}O$ values in the shells of the mollusk *M. donacium*, especially because of low sea water $\delta^{18}O$ variability along the central and southern coasts of Peru. We analyzed a modern sample of 13 shells from the Peruvian southern coast (Rio Ica, Fig. 1) that represents a modern reference to estimate past oceanographic changes. The mean seasonal amplitude of SST is estimated by the mean of ΔT values (<ΔT>) calculated from the shell sample. The seasonal amplitude of SST, ΔT, along the length of the Peruvian coast is strongly correlated with the El Niño1 + 2 index from 1950 to 2002. Therefore, the variance, Var(ΔT), calculated from a shell sample yields a reliable estimate of the amplitude of ENSO variability at the regional scale. This variability includes the range of anomalies from La Niña to moderate El Niño events, but excludes extreme warm anomalies like the 1997–98 event because of high mortality of the shells. $<\Delta T>_{fossil}/<\Delta T>_{modern}$ and $Var(\Delta T)_{fossil}/Var(\Delta T)_{modern}$ would yield quantitative estimates of past changes in SST seasonality and ENSO activity, and are

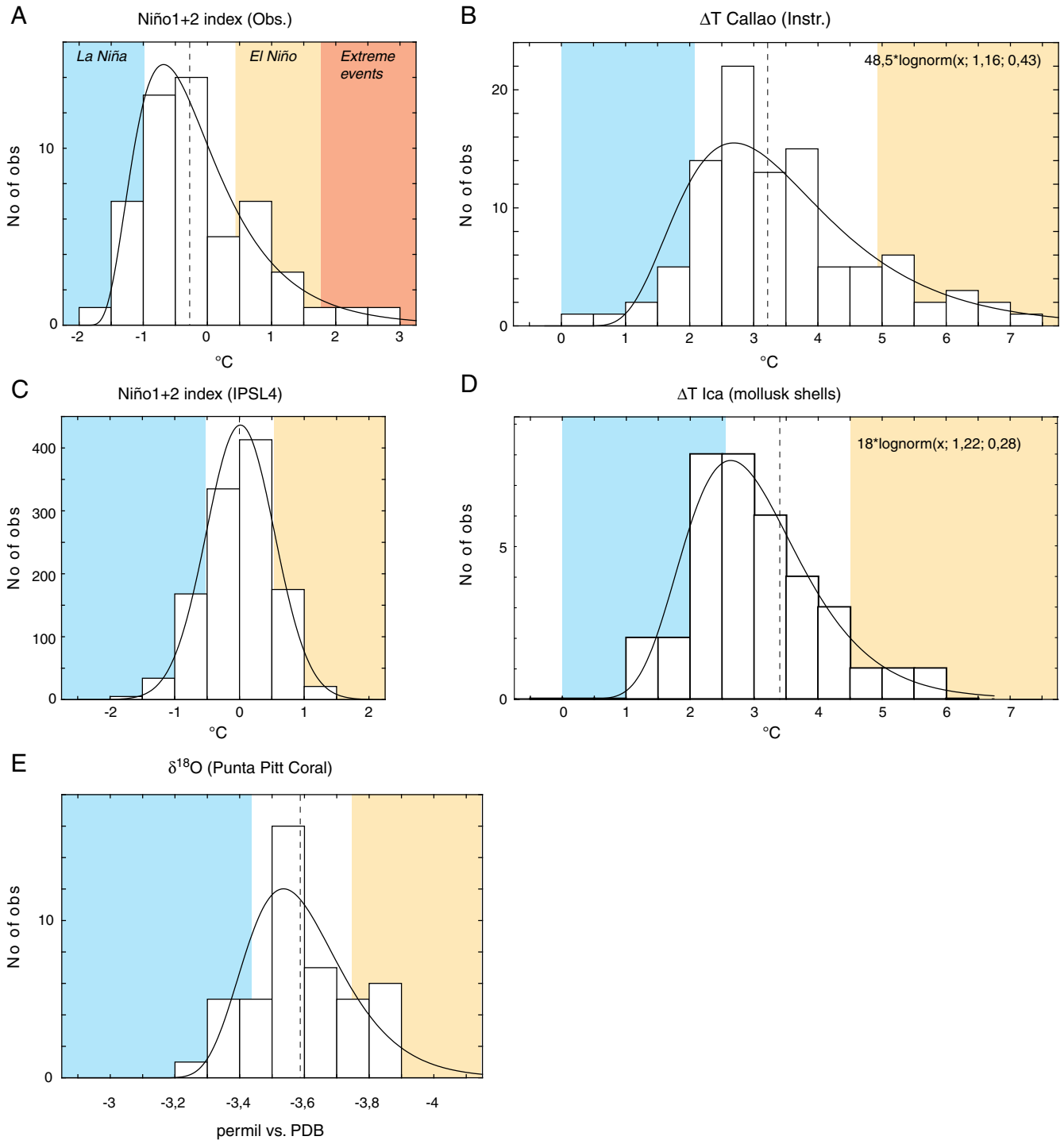

Fig. 7. Frequency distributions of (A) Niño1+2 index annual means from 1950 to 2002, (B) Callao ΔT values from 1950 to 2002, (C) Niño1+2 index annual means from IPSL_CM4v2 preindustrial control simulation, (D) ΔT values calculated from *M. donacium* shells from Rio Ica, (E) $\delta^{18}O$ annual means from the Punta Pitt coral recording the 1936–1982 period (Shen et al., 1992). Black curves represent the best lognormal fit, and the best normal fit for (C). Blue and yellow areas indicate La Niña and El Niño events respectively.

independent from the paleotemperature proxy model. The uncertainty of these reconstructions can be quantitatively estimated by the MoCo program (Carré et al., 2012). Changes in the event intensity and in the distribution of cold and warm ENSO events can be studied by the ΔT frequency distribution provided shell samples. The representation of ENSO activity as a frequency distribution of event intensity permits the comparison of shell records with coral records and with climate model simulations, which can give crucial insights into the variability of the spatial pattern of ENSO anomalies and the associated mechanisms. The method presented here may be used with any mollusk shell species that faithfully records the full annual cycle of SST. Well-preserved fossil mollusk shells are available in

abundance on the Peruvian coast for the Holocene period in anthropogenic shell middens or for the Pleistocene in marine terraces, and thus offer a unique opportunity to estimate quantitatively past ENSO activity in the eastern tropical Pacific.

Acknowledgments

This material is based upon work supported by the Joint Institute for the Study of Atmosphere and Ocean through a postdoctoral fellowship, the U.S. National Science Foundation under grant no. NSF-ATM-0811382 (J.P.S.), the U.S. National Oceanic and Atmospheric Administration under grant no. NOAA-NA08OAR4310685 (J.P.S.), and the ANR research project EL PASO (P.I. P. Braconnot). We are thankful to Catherine Pierre for water isotopic analyses. We thank 4 anonymous reviewers for helping improving the manuscript. This is ISEM contribution N° 2012-216.

Appendix A. Supplementary data

Supplementary data to this article can be found online at http://dx.doi.org/10.1016/j.palaeo.2012.12.014.

References

Andrus, C.F.T., Hodgins, G.W.L., Sandweiss, D.H., Crowe, D.E., 2005. Molluscan radiocarbon as a proxy for El Niño-related upwelling variation in Peru. In: Mora, G., Surge, D. (Eds.), Isotopic and Elemental Tracers of Cenozoic Climate Change. Geological Society of America, pp. 13–20.

Carré, M., 2007. El mes de recolección de la macha (Mesodesma donacium) determinado por sus líneas de crecimiento: aplicaciones arqueológicas. Bulletin de l'Institut Français d'Etudes Andines 36, 299–304.

Carré, M., Bentaleb, I., Blamart, D., Ogle, N., Cardenas, F., Zevallos, S., Kalin, R.M., Ortlieb, L., Fontugne, M., 2005. Stable isotopes and sclerochronology of the bivalve *Mesodesma donacium*: potential application to Peruvian paleoceanographic reconstructions. Palaeogeography, Palaeoclimatology, Palaeoecology 228, 4–25.

Carré, M., Klaric, L., Lavallée, D., Julien, M., Bentaleb, I., Fontugne, M., Kawka, O., 2009. Insights into early Holocene hunter-gatherer mobility on the Peruvian Southern Coast from mollusk gathering seasonality. Journal of Archaeological Science 36, 1173–1178.

Carré, M., Sachs, J.P., Wallace, J.M., Favier, C., 2012. Exploring errors in paleoclimate proxy reconstructions using Monte Carlo simulations: paleotemperature from mollusk and coral geochemistry. Climate of the Past 8, 433–450.

Cobb, K.M., Charles, C.D., Cheng, H., Edwards, R.L., 2003. El Niño/Southern Oscillation and tropical Pacific climate during the last millenium. Nature 424, 271–276.

Cohn, M., Urey, H.C., 1938. Oxygen exchange reactions of organic compounds with water. Journal of the American Chemical Society 60, 679–687.

Cole, J.E., Fairbanks, R.G., 1990. The southern oscillation recorded in the $\delta^{18}O$ of corals from Tarawa Atoll. Paleoceanography 5, 669–683.

Conroy, J.L., Overpeck, J.T., Cole, J.E., Shanahan, T.M., Steinitz-Kannan, M., 2008. Holocene changes in eastern Pacific climate inferred from a Galápagos lake sediment record. Quaternary Science Reviews 27, 1166–1180.

Coplen, T.B., 1996. New guidelines for reporting stable hydrogen, carbon, and oxygen isotope-ratio data. Geochimica et Cosmochimica Acta 60, 3359–3360.

Corrège, T., Delcroix, T., Rècy, J., Beck, W., Cabioch, G., Le Cornec, F., 2000. Evidence for stronger El Niño-Southern Oscillation (ENSO) events in a Mid-Holocene massive coral. Paleoceanography 15, 465–470.

D'Arrigo, R.D., Jacoby, G.C., 1992. A tree-ring reconstruction of New Mexico winter precipitation and its relation to El Niño/Southern Oscillation events. In: Diaz, H.F., Markgraf, V. (Eds.), El Niño, Historical and Paleoclimatic Aspects of the Southern Oscillation. Cambridge University Press, Cambridge, pp. 243–257.

D'Arrigo, R., Cook, E.R., Wilson, R.J., Allan, R., Mann, M.E., 2005. On the variability of ENSO over the past six centuries. Geophysical Research Letters 32.

Dunbar, R.B., Wellington, G.M., Colgan, M.W., Glynn, P.W., 1994. Eastern Pacific sea surface temperature since 1600 A.D.: the $\delta^{18}O$ record of climate variability in Galapagos corals. Paleoceanography 9, 291–315.

Epstein, S., Mayeda, T., 1953. Variation of ^{18}O content of waters from natural sources. Geochimica et Cosmochimica Acta 4, 213–224.

Evans, M.N., Kaplan, A., Cane, M.A., 2002. Pacific sea surface temperature field reconstruction from coral $\delta^{18}O$ data using reduced space objective analysis. Paleoceanography 17.

Fairbanks, R.G., Sverdlove, M., Free, R., Wiebe, P.H., Bé, A.W.H., 1982. Vertical distribution and isotopic fractionation of living planktonic foraminifera from the Panama basin. Nature 298, 841–844.

Garreaud, R.D., Vuille, M., Compagnucci, R., Marengo, J., 2009. Present-day South American climate. Palaeogeography, Palaeoclimatology, Palaeoecology 281, 180–195.

Grossman, E.L., Ku, Teh-Lung, 1986. Oxygen and carbon fractionation in biogenic aragonite: temperature effect. Chemical Geology 59, 59–74.

Hickson, J.A., Johnson, A.L.A., Heaton, T.H.E., Balson, P.S., 1999. The shell of the queen scallop *Aequipecten opercularis* as a promising tool for paleoenvironmental reconstruction: evidence and reasons for equilibrium stable-isotope incorporation. Palaeogeography, Palaeoclimatology, Palaeoecology 154, 325–337.

Jones, K.B., Hodgins, G.W.L., Etayo-Cadavid, M.F., Andrus, C.F.T., 2009. Upwelling signals in radiocarbon from early 20th-century Peruvian bay scallop (*Argopecten purpuratus*) shells. Quaternary Research 72, 452–456.

Kilbourne, K.H., Quinn, T.M., Taylor, F.W., Delcroix, T., Gouriou, Y., 2004. El Niño-Southern Oscillation-related salinity variations recorded in the skeletal geochemistry of a Porites coral from Espiritu Santo, Vanuatu. Paleoceanography 19, PA4002.

Kim, S.-T., Mucci, A., Taylor, B.E., 2007. Phosphoric acid fractionation factors for calcite and aragonite between 25 and 75 °C: revisited. Chemical Geology 246, 135–146.

Koutavas, A., deMenocal, P.B., Olive, G.C., Lynch-Stieglitz, J., 2006. Mid-Holocene El Niño-Southern Oscillation (ENSO) attenuation revealed by individual foraminifera in eastern tropical Pacific sediments. Geology 34, 993–996.

Lavallée, D., Julien, M., Béarez, P., Bolaños, A., Carré, M., Chevalier, A., Delabarde, T., Fontugne, M., Rodríguez-Loredo, C., Klaric, L., Usselmann, P., Vanhaeren, M., 2011. Quebrada de los burros. Los primeros pescadores del litoral Pacífico en el extremo sur peruano. Chungara, Revista de Antropología Chilena 43, 333–351.

Lazareth, C.E., Lasne, G., Ortlieb, L., 2006. Growth anomalies in *Protothaca thaca* (Mollusca, Veneridae) shells as markers of ENSO conditions. Climate Research 30, 263–269.

Leduc, G., Vidal, L., Cartapanis, O., Bard, E., 2009. Modes of eastern equatorial Pacific thermocline variability: implications for ENSO dynamics over the last glacial period. Paleoceanography 24. http://dx.doi.org/10.1029/2008PA001701.

McCulloch, M., Mortimer, G., Esat, T., Xianghua, L., Pillans, B., Chappell, J., 1996. High resolution windows into early Holocene climate: Sr/Ca coral records from the Huon Peninsula. Earth and Planetary Science Letters 138, 169–178.

McGregor, S., Timmermann, A., Timm, O., 2010. A unified proxy for ENSO and PDO variability since 1650. Climate of the Past 6, 1–17.

Monterey, G.I., Levitus, S., 1997. Climatological Cycle of Mixed Layer Depth in the World Ocean. U.S. Gov. Printing Office, NOAA NEDIS, p. 5.

Moy, C.M., Seltzer, G.O., Rodbell, D.T., Anderson, D.M., 2002. Variability of El Niño/Southern Oscillation activity at millennial timescales during the Holocene epoch. Nature 420, 162–165.

Perrier, C., Hillaire-Marcel, C., Ortlieb, L., 1994. Paléogéographie littorale et enregistrement isotopique (^{13}C, ^{18}O) d'évènements de type El Niño par les mollusques Holocènes et récents du Nord-Ouest Péruvien. Géographie Physique et Quaternaire 48, 23–38.

Rein, B., Lückge, A., Reinhardt, L., Sirocko, F., Wolf, A., Dullo, W.-C., 2005. El Niño variability off Peru during the last 20,000 years. Paleoceanography 20. http://dx.doi.org/10.1029/2004PA001099.

Riascos, J.M., Carstensen, D., Laudien, J., Arntz, W.E., Oliva, M.E., Güntner, A., Heilmayer, O., 2009. Thriving and declining: climate variability shaping life-history and population persistence of *Mesodesma donacium* in the Humboldt Upwelling System. Marine Ecology Progress Series 385, 151–163.

Riedinger, M.A., Steinitz-Kannan, M., Last, W.M., Brenner, M., 2002. A ~6100 ^{14}C yr record of El Niño activity from the Galapagos Islands. Journal of Paleolimnology 27, 1–7.

Rodbell, D.T., Seltzer, G.O., Anderson, D.M., Abbott, M.B., Enfield, D.B., Newman, J.H., 1999. An ~15,000-year record of El Niño driven alluviation in southwestern Ecuador. Science 283, 516–520.

Sandweiss, D.H., Richardson III, J.B., Reitz, E.J., Hsu, J.T., Feldman, R.A., 1989. Early maritime adaptations in the Andes: preliminary studies at the Ring Site, Peru. In: Rice, D., Stanish, C., Scarr, P.R. (Eds.), Ecology, Settlement and History in the Osmore Drainage, Peru: BAR International Series, 545 (i), pp. 35–84 (Oxford, I).

Sandweiss, D.H., McInnis, H., Burger, R.L., Cano, A., Ojeda, B., Paredes, R., Sandweiss, M.C., Glascock, M.D., 1998. Quebrada Jaguay: South American maritime adaptations. Science 281, 1830–1832.

Schöne, B.R., Freyre Castro, A.D., Fiebig, J., Houk, S.D., Oschmann, W., Kröncke, I., 2004. Sea surface water temperatures over the period 1884–1983 reconstructed from oxygen isotope ratios of a bivalve mollusk shell (*Arctica islandica*, southern North Sea). Palaeogeography, Palaeoclimatology, Palaeoecology 212, 215–232.

Servonnat, J., Yiou, P., Khodri, M., Swingedouw, D., Denvil, S., 2010. Influence of solar variability, CO2 and orbital forcing between 1000 and 1850 AD in the IPSLCM4 model. Climate of the Past 6, 445–460.

Shen, G.T., Cole, J.E., Lea, D.W., Linn, L.J., McConnaughey, T.A., Fairbanks, R.G., 1992. Surface ocean variability at Galapagos from 1936–1982: calibration of geochemical tracers in corals. Paleoceanography 7, 563–588.

Stahle, D.W., D'Arrigo, R.D., Krusic, P.J., Cleaveland, M.K., Cook, E.R., Allan, R.J., Cole, J.E., Dunbar, R.B., Therrell, M.D., Gay, D.A., Moore, M.D., Stokes, M.A., Burns, B.T., Villanueva-Diaz, J., Thompson, L.G., 1998. Experimental dendroclimatic reconstruction of the Southern Oscillation. Bulletin of the American Meteorological Society 79, 2137–2152.

Takahashi, K., Montecinos, A., Goubanova, K., Dewitte, B., 2011. ENSO regimes: reinterpreting the canonical and Modoki El Niño. Geophysical Research Letters 38.

Tarifeño, E., 1980. Studies on the Biology of Surf Clam *Mesodesma donacium* (Lamarck, 1818) (Bivalvia: Mesodesmatidae) from Chilean Sandy Beaches. University of California, Los Angeles, p. 229.

Tobin, T.S., Schauer, A.J., Lewarch, E., 2011. Alteration of micromilled carbonate $\delta^{18}O$ during Kiel Device analysis. Rapid Communications in Mass Spectrometry 25, 2149–2152.

Tudhope, A.W., Chilcott, C.P., McCulloch, M.T., Cook, E.R., Chappell, J., Ellam, R.M., Lea, D.W., Lough, J.M., Shimmield, G.B., 2001. Variability in the El-Niño Southern Oscillation through a Glacial–Interglacial Cycle. Science 291, 1511–1517.